LOCKHEED MARTIN ENERGY RESEARCH LIBRARIES
3 4456 0514422 4

CENTRAL RESEARCH LIBRARY
DOCUMENT COLLECTION

OAK RIDGE NATIONAL LABORATORY
operated by
UNION CARBIDE CORPORATION
for the
U.S. ATOMIC ENERGY COMMISSION

ORNL-TM-3521
Cy 20

DATE - August 1, 1971

Neutron Physics Division

FAST REACTOR SHIELDING MONTHLY PROGRESS REPORT FOR JUNE, 1971, 189A No. 10028, ACTIVITY NO. 40 01 61

Report Written By:

M. L. Gritzner
J. Lewin
R. E. Maerker
F. R. Mynatt
P. N. Stevens*

Work Done By:

R. M. Freestone, Jr.
M. L. Gritzner
K. M. Henry, Jr.
J. L. Hull
J. Lewin
R. E. Maerker
J. J. Manning
J. N. Money
F. J. Muckenthaler
L. R. Williams
W. Zobel

OAK RIDGE NATIONAL LABORATORY
CENTRAL RESEARCH LIBRARY
DOCUMENT COLLECTION
LIBRARY LOAN COPY
DO NOT TRANSFER TO ANOTHER PERSON
If you wish someone else to see this document, send in name with document and the library will arrange a loan.
UCN-7969
(3-67)

Abstract

This report summarizes the progress made by the ORNL Neutron Physics Division in Fast Reactor Shielding Research during the month of June 1971.

*University of Tennessee, Knoxville, Tennessee.

NOTICE This document contains information of a preliminary nature and was prepared primarily for internal use at the Oak Ridge National Laboratory. It is subject to revision or correction and therefore does not represent a final report.

This report was prepared as an account of work sponsored by the United States Government. Neither the United States nor the United States Atomic Energy Commission, nor any of their employees, nor any of their contractors, subcontractors, or their employees, makes any warranty, express or implied, or assumes any legal liability or responsibility for the accuracy, completeness or usefulness of any information, apparatus, product or process disclosed, or represents that its use would not infringe privately owned rights.

Monthly Progress Report

JUNE 1971

FAST REACTOR SHIELDING
Activity No. 40 01 61
189A No. 10028

Approved by:

Fred R. Mynatt
Head, Reactor Shielding Program

C. E. Clifford
Associate Division Director

LOCKHEED MARTIN ENERGY RESEARCH LIBRARIES

3 4456 0514422 4

TABLE OF CONTENTS

	Page
SCHEDULE FOR FY-1971 EXPERIMENTS	v
ANALYTICAL CALCULATIONS EFFORT	vi
LIST OF FIGURES	vii
LIST OF TABLES	viii
A. TRANSPORT METHOD DEVELOPMENT FOR ALL METAL SHIELDS	1
1. TSF ANNULAR SLIT EXPERIMENT - DISCRETE ORDINATES ANALYSIS	1
B. CURRENT FFTF STUDIES	4
1. VESSEL SUPPORT SYSTEM STREAMING	4
2. GRID-PLATE SHIELD ANALYSIS	5
3. GAMMA-RAY STREAMING IN HEAD	7
C. MONTE CARLO TRANSPORT THROUGH IRON (IRON BENCHMARK)	8
D. ORNL-LMFBR EXPERIMENTAL SHIELDING PROGRAM AT THE TSF	15
1. PROTOTYPE BOTTOM SHIELD EXPERIMENT	15
a. EXPERIMENTAL CONFIGURATION	15
b. RESULTS	16
2. BULK SODIUM EXPERIMENT	16

ORNL-LMFBR SHIELDING PROGRAM (1970/1971)
Schedule for FY-1971 Experiments

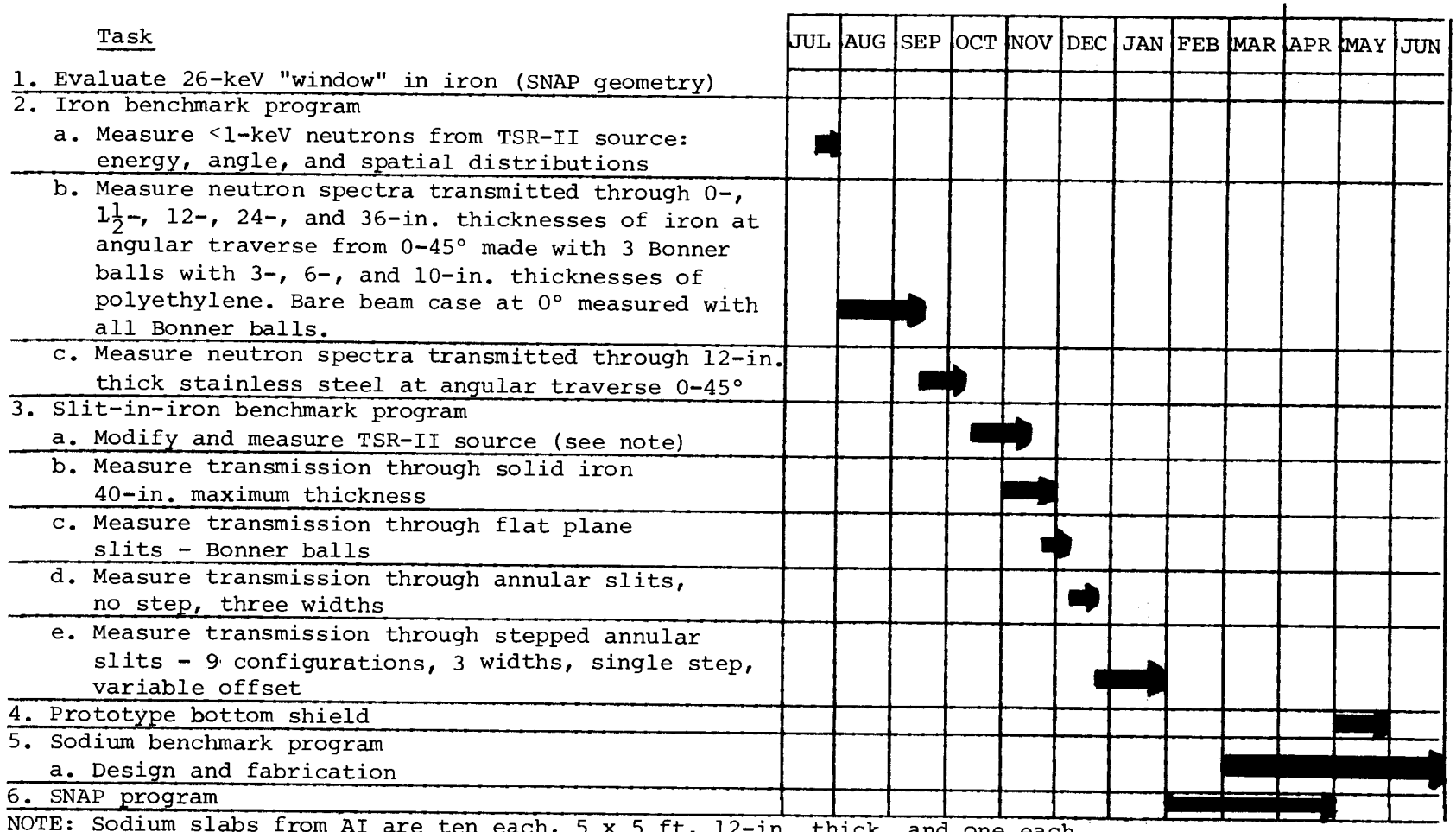

NOTE: Sodium slabs from AI are ten each, 5 x 5 ft, 12-in. thick, and one each, 5 x 5 ft, 6-in. thick. Walls are 1/4-in. 6061T6 aluminum.

Spectral measurements made with: (1) Source - TSR-II, 15-in. diam. beam hole, (2) NE-213 scintillator for 0°, 6-in. and 12-in. thicknesses, (3) Blosser spectrometer for 1/2- and 1-1/2-in. thicknesses, (4) Bonner balls for 1-1/2, 12, 24, and 36 in., (5) Hydrogen counter for bare beam measurements (0 thickness) 14 ft from end of collimator at 0°, and 12-in. iron and 12-in. stainless steel, 12 in. off centerline with detector at slab surface.

ORNL-LMFBR SHIELDING PROGRAM (1970/1971)
Analytical Calculations Effort

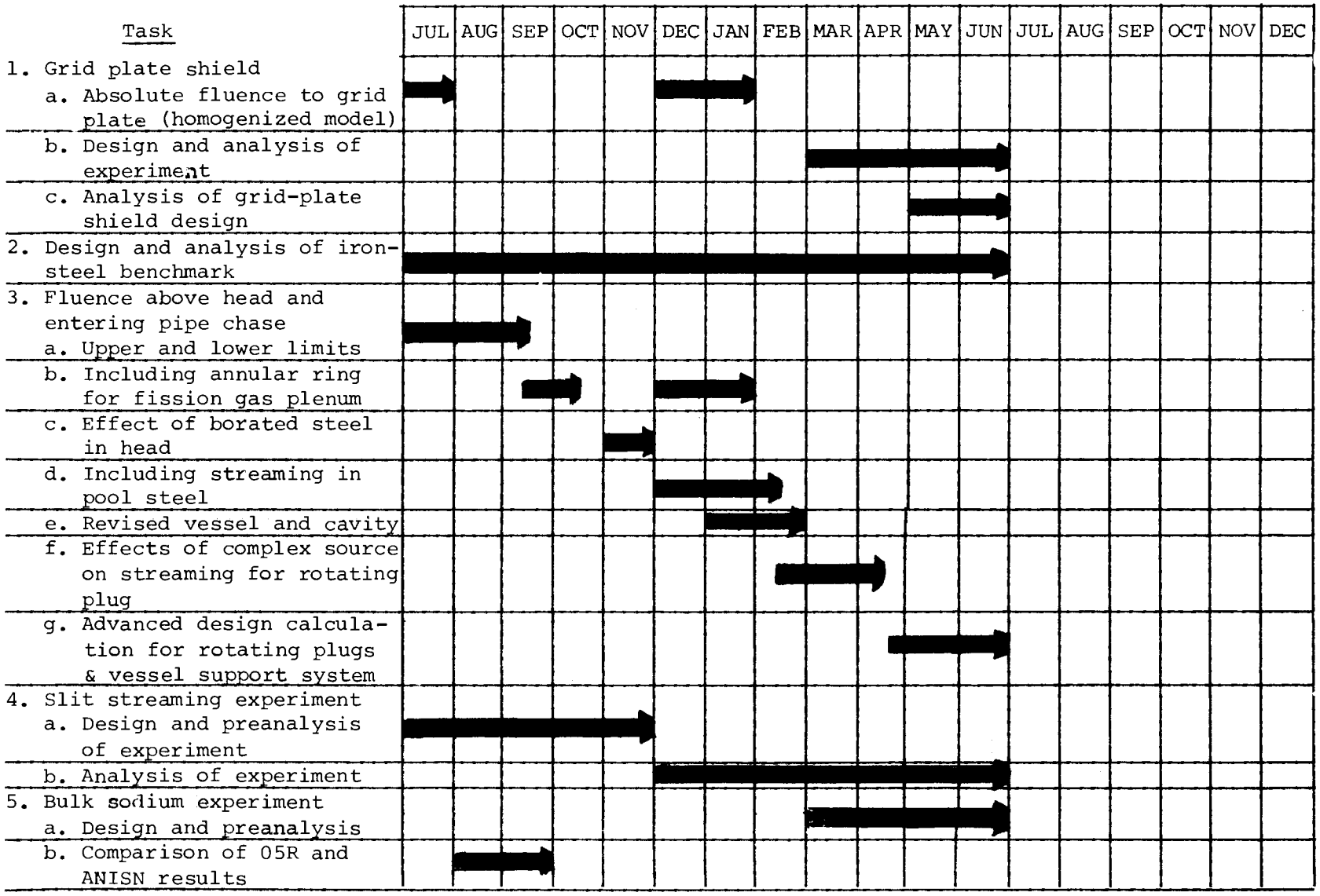

NOTE: Duct Streaming Analysis to be rescheduled.

LIST OF FIGURES

Page

Fig. 1. Experimental Configuration No. 1 18

Fig. 2. Modified Configuration No. 1 19

Fig. 3. Comparison of Unfolded Hydrogen Counter Spectra With ANISN Calculations. 20

Fig. 4. Comparison of Unfolded NE-213 Spectra With ANISN Calculations 21

LIST OF TABLES

Page

Table 1. Summary of Measured/Calculated Ratios for Traverse Integral of 3- and 6-in. Bonner Ball Detectors for Annular Slit Configurations 2

Table 2. Grid-Plate Shield Model. 6

Table 3. Comparison of Calculated and Measured Fluxes Behind 12 in. of Iron on Centerline 10 in. Behind Slab 9

Table 4. Comparison of Calculated and Measured Fluxes Behind 12 in. of Iron, 10 in. Behind Slab, and 12 in. Off Centerline . . . 10

Table 5. Comparison of Calculated and Measured Fluxes Behind 12 in. of Stainless Steel on Centerline 10 in. Behind Slab. 11

Table 6. Comparison of Calculated and Measured Fluxes Behind 12 in. of Stainless Steel, 10 in. Behind Slab, and 12 in. Off Centerline. 12

Table 7. Comparison of Calculated and Measured Bonner Ball Responses Behind 12 in. of Stainless Steel in Counts/Min/kW 14

Table 8. ANISN Modified-Source Calculations 22

Table 9. Calculated Bonner Ball Count Rates Vs. Measured for SNAP Spectrum Modifier, 10-in. Stainless Steel + 1-in. Poly. + 1/4-in. Boral 23

A. Transport Method Development For All Metal Shields

1. TSF Annular Slit Experiment - Discrete Ordinates Analysis

A summary of the annular slit calculations performed to date is given in Table 1. Pertinent information concerning the calculations and comparisons of measured/calculated ratios for the integrals of the 3- and 6-in. Bonner ball traverses is also presented. The calculated results were obtained as a spatial distribution for a point detector at the center of each ball having a response of the finite Bonner ball. The recalculated 100-group response functions (see May 1971 Monthly Progress Report) were used, together with the experimentally determined efficiencies of the 3- and 6-in. Bonner ball detectors - 0.457 and 0.418, respectively. It must be noted that the integrals of the calculated results used in the measured/calculated ratios shown for each of the configurations in Table 1 are corrected values in that the calculated results in previously reported measured/calculated ratios were obtained with integration over a slightly larger area of the annular assembly than the integrals for the measured results. The integrals of the measured count rate have also been corrected for background. For the ratios shown in Table 1, a background of 120 cpm/100 kW was assumed for the 3-in. Bonner ball traverse and 200 cpm/100 kW for the 6-in. Bonner ball measurements. These background levels were obtained as the minima of the measured 3- and 6-in. Bonner ball traverses for the solid annular assembly with collimators of various annular slit thicknesses (Tables 16 and 17, January 1971 Monthly Progress Report).

Several observations may be made from the results shown in Table 1. Considering the calculated results for which the S_{298} quadrature set and the Penny iron cross sections were used, the 3-in. Bonner ball integrals

Table 1. Summary of Measured/Calculated Ratios for Traverse Integral of 3- and 6-in. Bonner Ball Detectors for Annular Slit Configurations

Configurations		Cross Sections (50 groups, P_1 Expansion)	Number of Angles	3-in. Bonner Ball Integral Ratio	6-in. Bonner Ball Integral Ratio
3/4-in. straight slit with no collimator	1a	Irving	315	1.17	1.76
	1b*	Penny	315	1.04	1.45
	1c*	Penny	298	0.95	1.36
3/4-in. straight slit with collimator**	2a	Irving	315	1.05	1.41
	2b	Penny	298	0.94	1.26
3/4-in. slit with 3/4-in. offset with collimator	3a	Irving	315	1.40	1.82
	3b*	Penny	315	1.13	1.51
	3c*	Penny	298	0.99	1.32
solid annular assembly with no collimator	4a	Irving	315	-	2.72
	4b	Penny	315	-	1.81
solid annular assembly with collimator	5*	Penny	298	1.05	1.27

*These calculations performed in June 1971 with the DOT-II code.

**Collimator is 4-in. lucite polyethylene with 9/8-in. wide annular slit.

agree very well with the measured values for all of the configurations. The calculated 6-in. Bonner ball integrals are 26% to 36% lower than the measured integrals for all of the configurations, except the solid annular assembly with no collimator (configuration 4b in Table 1) for which the calculated result is 80% lower than the measured result. Disregarding the results for configuration 4b for the moment, it will be noted that this discrepancy between the measured and calculated ratios for the 3- and 6-in. Bonner balls is consistent with the Monte Carlo results for 36 in. of iron previously reported for the iron benchmark experiment (May 1971 Monthly Progress Report). Additionally, the increase in the calculated results using the S_{298} quadrature versus the S_{315} quadrature for configurations 1c and 3c agrees favorably with the results of the annular slit quadrature study reported last month.

The 80% disagreement for the 6-in. Bonner ball integrals for the solid annular assembly with no collimator is quite puzzling in view of the 6-in. Bonner ball results for the same assembly but with the collimator. This apparent anomaly may be due to the assumed background of 200 cpm/100 kW for the 6-in. Bonner ball detector traverse. If, for instance, the background is assumed to be on the order of 150 cpm/100 kW, then the 27% error in the 6-in. Bonner ball results for configuration no. 5 would become 75%, since it appears that the background, whatever it may be, is approximately half of the measured integral count rate for this configuration. If this is so, then the 6-in. Bonner ball comparisons for the solid annular assembly with and without the collimator become more reasonable. Continued investigation concerning the background will be made.

Annular slit analysis efforts next month will include investigation of two other possible sources of error in the calculations performed to date.

These are (1) the neutron transport in the upper keV energy region (specifically in the solid annular assembly with no collimator), and (2) a recalculation of the TSR-II beam modifier (consisting of 8 in. of iron followed by 5 ft of sodium in aluminum cans) using the Penny iron cross sections and the preliminary version of the ENDF/B-III sodium cross sections. In addition, a 3/4-in. slit with a 1 1/2-in. offset with the collimator will be calculated.

B. Current FFTF Studies

1. Vessel Support System Streaming

Two-dimensional calculations were completed for the problem of estimating the effectiveness of a shield deck in the reactor cavity. Last month's report included the results of a core-to-cover r-z calculation with a 12-in.-thick B_4C shield deck in the reactor cavity at the top of the guard vessel and extending from the guard vessel to the concrete wall. The effect of the shield deck on the vessel support system streaming problem was determined by coupling the core-to-cover r-z calculation to the head streaming calculation. The model for the vessel support system streaming calculation was that described in the letter dated 2-23-71, ref. FPS-940, from Fox to Mynatt, and the coupling procedure was the same as that described in the 5-11-71 letter from Mynatt to Fox.

The results of this calculation showed that the shield deck was very effective in that the peak total neutron flux above the vessel support area was 5.08×10^0 neutrons/cm^2/sec compared with the previous results of 8.59×10^2 neutrons/cm^2/sec without the shield deck. This reduction by a factor of 169 is very large compared to the effects on total flux and spectra observed in the cavity and the amplification must be due to the combined effect on

spectra and spacial and angular distribution of the cavity flux. As mentioned previously, the shield deck is too thick and a cheaper and/or thinner shield would give the same effect. Also, the calculated effect is optimistic since the shield deck does not include the pipe penetrations.

2. Grid-Plate Shield Analysis

The grid-plate shield problem for the FTR still commands considerable interest since the present calculations indicate a grid lifetime less than ten years. The TSF prototype grid-plate shield streaming experiment reported last month showed that streaming effects were small, i.e., on the order of 1.03 to 1.04 streaming factors for insert 2 which had a single offset. Since the experiment did not contain a fully homogenized insert, a DOT calculation of the FTR below-core configuration was performed using a four-zone grid-shield mockup which corresponded to the prototype insert 3. The shield description is given in Table 2.

The new calculation gave 4.09×10^{13} neutrons/cm^2/sec as the peak flux in the topmost axial interval in the grid plate compared to 3.96×10^{13} neutrons/cm^2/sec previously obtained for a fully homogenized grid-plate shield. The peak flux on the surface of the grid plate obtained by interpolation is 4.24×10^{13} neutrons/cm^2/sec in the new four-zone calculation. Using 1.04 as the streaming factor, the peak flux on the grid plate is estimated to be 4.41×10^{13} neutrons/cm^2/sec. For a total fluence limit of 9.5×10^{21} neutrons/cm^2, the grid-plate lifetime is 9.76 years at 70% availability. The magnitude of the uncertainty in the calculation due to cross-section treatment is unknown, but the nature of the approximations is such that the present calculation is optimistic and an improved calculation will indicate a shorter life. On the other hand, Rathbun indicates that it may be possible

Table 2. Grid-Plate Shield Model

Zone	Outer Radius	Volume % SS-304	Volume % Na
1	4.722 cm	55.8	44.2
2	7.262	77.3	22.7
3	16.693	64.6	35.4
4	60.000	75.0	25.0

to further increase the steel volume fraction such as to obtain a longer life. An indication of the sensitivity to cross sections will be obtained by repeating the DOT calculation with the Penny evaluation for iron replacing the Irving evaluation. The Irving evaluation is presently being used with 1/E σ_T weighting for the iron and 1/E weighting for the other elements rather than 1/E σ_T weighting for the mixture as will be done in the future. An indication of the absolute accuracy of the calculations will be given by analysis of the TSF grid-plate shield experiment.

3. Gamma-Ray Streaming in Head

In considering the choice between a single offset or double offset for the rotating plug clearance gaps, several of the present design alternatives such as a cavity shield deck or additional shielding in the vessel support system enhance the case for a single offset while other alternatives such as reduction of thermal shield thickness and uncertainties in the effect of stored fuel and of gamma-ray streaming may lead to double offsets and narrower clearances. The possibility of gamma-ray streaming in the single offset plug geometry was investigated by performing a DOT calculation with the following characteristics:

(a) The boundary condition was described as an isotropic flux of 2.75 and 1.38-MeV gamma rays which is a cosine source having an intensity of 10^{10} gammas/cm^2/sec in each of the two sodium lines placed beneath the thermal shield.

(b) The single offset annular slit (29-in.-long, 1/2-in.-wide slit followed by a 17-in.-long, 3/8-in.-wide slit) followed by the massive plug-head interface flange described by the letter FPS-1103 from Fox to Mynatt. The r-z geometry was described by 2720

space points and the S_{315} quadrature was used.

(c) The cross sections came from the MUG code with 18 groups used and the angular distribution described by a P_3 expansion with a P_4 consistent transport correction for within-group scattering.

(d) 360/91 CPU execution time of 59 min.

The calculation showed considerable streaming with gamma-ray doses above the head being 19 mr/hr at the slit and 7×10^{-3} mr/hr at the center of the plug. The massive flange, however, was very effective in further reducing the observed gamma-ray dose levels. Across the top of the flange the maximum dose rate was 8×10^{-3} mr/hr and along the side of the flange the maximum dose rate was 6×10^{-2} mr/hr due to scattering at the end of the 3/8-in. slit in the flange.

Work is continuing on the secondary gamma-ray analysis, the reduction of conservatism in the fission gas plenum calculations, and the study of the effect of stored fuel.

C. Monte Carlo Transport Through Iron (Iron Benchmark)

A recent improvement in SPEC-4 has led to a reunfolding of the experimental hydrogen counter results behind 12 in. of iron and 12 in. of stainless steel. The measured fluxes are now $\sim$ 10% higher than those obtained earlier. In addition, MORSE problems were run for 12 in. of stainless steel using a 218-group P_3 set of cross sections derived from the Penny iron evaluation and ENDF/B-I data on manganese, chromium, and nickel. Tables 3-6 present the comparisons between calculations and experiment.

A comparison of the stainless steel with the iron results shows that the flux in the hydrogen counter region is reduced by only a factor of 0.67 on

Table 3. Comparison of Calculated and Measured Fluxes Behind 12 in. of Iron on Centerline 10 in. Behind Slab

ΔE (keV)	ϕ (neut/cm^2/min/kW) Measured	Calculated Free Field	Calculated Albedo Enhancement	Calculated Sum	Calc/Meas
1270-1500	6.58+3*	3.54+3	3.4+1	3.57+3	0.60
1082-1270	9.06+3	5.71+3	8.0+1	5.79+3	
915-1082	1.017+3	6.63+3	1.0+2	6.73+3	0.64
785-915	8.84+3	5.37+3	1.6+2	5.53+3	
664-785	1.720+4	9.00+3	3.1+2	9.31+3	0.88
562-664	1.770+4	2.018+4	1.13+3	2.131+4	
478-562	1.049+4	9.94+3	9.2+2	1.086+4	0.99
434-478	5.59+3**	4.69+3	4.4+2	5.13+3	
365-434	1.495+4	8.05+3	8.9+2	8.94+3	1.02
314-365	1.771+4	2.163+4	2.77+3	2.440+4	
267-314	1.558+4	1.428+4	2.38+3	1.666+4	1.04
224-267	9.60+3	7.99+3	1.51+3	9.50+3	
190-224	7.89+3	5.89+3	1.10+3	6.99+3	1.01
179-190	3.22+3**	3.56+3	7.0+2	4.26+3	
153-179	9.41+3	1.140+4	2.31+3	1.371+4	1.20
129-153	1.118+4	7.74+3	1.70+3	9.44+3	
110-129	3.67+3	4.64+3	1.37+3	6.01+3	
93.6-110	2.49+3	3.91+3	1.19+3	5.10+3	1.30
79.4-93.6	3.42+3	1.95+3	6.2+2	2.57+3	
Totals	1.848+5	1.561+5	1.97+4	1.758+5	0.95

*Read as 6.58×10^3.

**Average over two counters in an overlap region.

Table 4. Comparison of Calculated and Measured Fluxes Behind 12 in. of Iron, 10 in. Behind Slab, and 12 in. Off Centerline

ΔE (keV)	ϕ (neut/cm^2/min/kW) Measured	Calculated Free Field	Calculated Albedo Enhancement	Calculated Sum	Calc/Meas
1106-1300	2.09+3*	1.50+3	4.2+1	1.54+3	0.73
939-1106	2.82+3	1.84+3	4.5+1	1.89+3	
791-939	3.38+3	2.54+3	1.2+2	2.66+3	
680-791	5.17+3	3.06+3	1.6+2	3.22+3	0.90
578-680	7.17+3	7.30+3	5.9+2	7.89+3	
486-578	5.76+3	5.93+3	5.4+2	6.47+3	1.07
412-486	4.69+3	4.31+3	4.4+2	4.75+3	
356-412	5.47+3	3.69+3	4.4+2	4.13+3	1.24
337-356	2.44+3**	4.19+3	7.2+2	4.91+3	
286-337	8.64+3	9.69+3	1.73+3	1.142+4	
243-286	5.79+3	5.76+3	1.08+3	6.84+3	1.11
210-243	3.75+3	3.14+3	6.1+2	3.75+3	
176-210	4.42+3	4.39+3	9.4+2	5.33+3	1.48
150-176	3.70+3	5.78+3	1.36+3	7.14+3	
144-150	1.18+3**	1.03+3	2.8+2	1.31+3	
123-144	4.39+3	3.38+3	9.1+2	4.29+3	1.26
104-123	1.79+3	2.67+3	8.2+2	3.49+3	
88-104	1.92+3	1.93+3	6.1+2	2.54+3	1.18
74-88	2.24+3	1.76+3	6.0+2	2.36+3	
Totals	7.68+4	7.39+4	1.20+4	8.59+4	1.12

*Read as 2.09×10^3.

**Average over two counters in an overlap region.

Table 5. Comparison of Calculated and Measured Fluxes Behind 12 in. of Stainless Steel on Centerline 10 in. Behind Slab

ΔE (keV)	ϕ(neut/cm^2/min/kW) Measured	Calculated Free Field	Calculated Albedo Enhancement	Calculated Sum	Calc/Meas
1268-1500	4.15+3*	2.94+3	3.3+1	2.97+3	0.71
1082-1268	5.62+3	3.94+3	4.5+1	3.99+3	
915-1082	6.67+3	4.71+3	8.2+1	4.79+3	0.72
785-915	6.24+3	4.41+3	1.4+2	4.55+3	
664-785	9.84+3	6.74+3	3.1+2	7.05+3	0.68
562-664	1.095+4	6.73+3	3.2+2	7.05+3	
478-562	7.92+3	6.76+3	3.9+2	7.15+3	0.88
431-478	4.37+3**	3.35+3	2.7+2	3.62+3	
366-431	8.36+3	5.29+3	3.5+2	5.64+3	0.78
314-366	1.090+4	8.62+3	8.3+2	9.45+3	
266-314	1.140+4	8.31+3	9.3+2	9.24+3	0.90
227-266	6.62+3	6.29+3	7.4+2	7.03+3	
193-227	4.76+3	4.76+3	5.7+2	5.33+3	1.11
179-193	2.21+3**	2.56+3	3.4+2	2.90+3	
153-179	5.68+3	5.09+3	6.8+2	5.77+3	
129-153	8.72+3	3.68+3	4.7+2	4.15+3	0.87
110-129	3.64+3	5.68+3	9.4+2	6.62+3	
93.6-110	2.52+3	3.43+3	6.0+2	4.03+3	1.23
79.4-93.6	3.40+3	2.76+3	4.8+2	3.24+3	
Totals	1.240+5	9.605+4	8.52+3	1.045+5	0.84

*Read as 4.15×10^3.

**Average over two counters in an overlap region.

Table 6. Comparison of Calculated and Measured Fluxes Behind 12 in. of Stainless Steel, 10 in. Behind Slab, and 12 in. Off Centerline

ΔE (keV)	ϕ (neut/cm^2/min/kW) Measured	Calculated Free Field	Calculated Albedo Enhancement	Calculated Sum	Calc/Meas
1106-1300	1.81+3*	1.20+3	1.4+1	1.21+3	0.76
939-1106	2.42+3	1.74+3	3.5+1	1.78+3	
791-939	2.73+3	2.22+3	9.0+1	2.31+3	
680-791	3.77+3	2.82+3	1.3+2	2.95+3	0.74
578-680	5.19+3	3.47+3	2.1+2	3.68+3	
486-578	4.62+3	3.54+3	1.8+2	3.72+3	0.76
412-486	3.77+3	2.50+3	1.7+2	2.67+3	
356-412	4.34+3	2.62+3	1.6+2	2.78+3	0.76
339-356	1.66+3**	1.50+3	2.4+2	1.74+3	
286-339	6.38+3	4.45+3	4.9+2	4.94+3	
243-286	4.79+3	3.52+3	4.0+2	3.92+3	0.98
208-243	2.79+3	3.14+3	3.6+2	3.50+3	
177-208	2.56+3	2.49+3	3.0+2	2.79+3	0.97
151-177	2.70+3	2.47+3	3.2+2	2.79+3	
144-151	1.16+3**	5.82+2	5.3+1	6.35+2	
122-144	4.12+3	2.44+3	3.1+2	2.75+3	1.00
103-122	1.68+3	2.68+3	3.9+2	3.07+3	
89.2-103	1.91+3	1.52+3	2.2+2	1.74+3	0.91
74.9-89.2	2.22+3	1.73+3	3.0+2	2.03+3	
Totals	6.06+4	4.663+4	4.37+3	5.10+4	0.84

*Read as 1.81×10^3.

**Average over two counters in an overlap region.

the centerline and 0.79 off the centerline, a rather surprising result since all of the windows in the iron are essentially wiped out by the chromium and nickel in the stainless steel. However, the uncollided contribution is small for the centerline detector (∿20% for iron, ∿5% for stainless steel) so that this reduction does not include much effect from the uncollided flux. The calculations are in good agreement with the measurements, being within ∿ ± 15% for both the iron and the stainless steel. The bracketing of the groups in the last column in the tables is an attempt at smoothing the experimental data; however, even without the bracketing there is general agreement with the calculations. The trend of the comparisons for both the iron and the stainless steel is that the calculations are low by about 30% in the region above ∿0.8 MeV and high by about 20% below ∿0.1 MeV; between ∿0.1 and 0.8 MeV the agreement is remarkably good. In the stainless-steel calculations reported above, "point" total cross sections were incorporated in MORSE for use in sampling collision sites and in next-flight estimation; they were not used in calculating the uncollided flux since this component is a very small part of the total flux.

Calculations were also made of the Bonner ball responses behind 12 in. of stainless steel, using the response functions corrected for efficiency described in last month's progress report. The "point" total cross-section data were used in these calculations to obtain the uncollided component on the centerline as well as for collision site sampling and next-flight estimation. The results and comparisons with experiment are presented in Table 7.

The agreement is not as good as that behind 12 in. of iron (see last month's progress report). There appears to be a disagreement in the

Table 7. Comparison of Calculated and Measured Bonner Ball Responses Behind 12 in. of Stainless Steel in Counts/Min/kW

	3-in. Bonner Ball			6-in. Bonner Ball			10-in. Bonner Ball		
	CL	15°	45°	CL	15°	45°	CL	15°	45°
Calculated	0.589	0.483	0.305	3.67	2.33	1.44	2.08	0.98	0.587
Measured	0.783	0.496	0.327	5.97	2.74	1.77	3.51	1.28	0.797
Calc/Meas	0.75	0.975	0.93	0.61	0.85	0.81	0.595	0.765	0.74

uncollided flux (as in iron), which is not necessarily limited to the region ~100 keV to 1 MeV, as in the case of iron, since the 3-in. Bonner ball centerline ratio is also low. The implication is that the nickel and/or chromium cross sections are not known nearly as well as those of iron, or that errors exist in the location of the windows in iron relative to the structure in the nickel and/or chromium. A third possibility that will be checked is that the density of the stainless steel is not the assumed handbook value of 7.88 grams/cm^3 but something less. The calculated uncollided fraction of the total flux incident on the centerline at the Bonner ball location is 0.35 behind the stainless steel and 0.77 behind 12 in. of iron. Comparing the measured counting rates behind the steel relative to the iron, the reduction factors are approximately 0.33 on the centerline, 0.82 at 15°, and 0.77 at 45°, the latter two comparing well with the hydrogen counter measurements.

D. ORNL-LMFBR Experimental Shielding Program at the TSF

1. Prototype Bottom Shield Experiment

Item 4 in the Schedule, the Prototype Bottom Shield experiments, was completed early in June. The measurements performed in June which were not reported in the May monthly progress report included the hydrogen counter and NE-213 spectral measurements of the modified source.

a. Experimental Configuration

The source of neutrons for these experiments was provided by the SNAP reactor. The desired incident spectrum on the grid-plate shield mock-up was obtained with the insertion of an appropriate "spectrum modifier," which consisted of 10 in. of stainless steel followed by 1 in. of plain

polyethylene and two 1/8-in. boral sheets. The design of the spectrum modifier was reported in the monthly progress report for April. The experimental setup (configuration no. 1) for the hydrogen counter measurement is the same used for the Bonner ball spectral measurement (as reported in the May 1971 monthly progress report) and is shown in Fig. 1. The hydrogen counter is located 5-11/32 in. below the spectrum modifier. The experimental setup of configuration no. 1 was changed by the inclusion of 1-15/16 in. Zr to reduce the gamma-ray intensity for the NE-213 spectral measurement. This modified configuration no. 1 is shown in Fig. 2.

b. Results

The measurements show that the emergent radiation from the SNAP reactor was modified to provide the desired source spectrum. Bonner ball measurements were taken during May, and additional spectral measurements were taken in June with the hydrogen counter and NE-213 spectrometers. The unfolded hydrogen counter spectrum and the NE-213 spectrum are plotted in Figs. 3 and 4, respectively. Also shown on these plots are calculated ANISN results. The ANISN spectrum, presented in Table 8, was normalized to the experimental spectra at 1 MeV so that the comparisons presented are of the spectrum shape only. Table 9 shows the comparison of measured and calculated Bonner ball count rates under the spectral modifier. The ANISN calculation is normalized to the experiment for the 5-in. Bonner ball.

2. Bulk Sodium Experiment

During June the first tank for the FFTF bulk sodium neutron transmission measurements was leak checked, purged with argon gas and filled with sodium. Cooling of the tank and its sodium contents was completed on June 25, 1971. Tank 4 was positioned for filling and as the month ended purging and preheating were under way.

The concrete caps for tanks 2 and 3 were poured, thus completing the concrete cap fabrication for all four tanks. Cap 2 was proof tested on June 2 for integrity of the lifting structure. The cap was picked up by the lifting fixture and was swung in a 90° arc to simulate loads that would occur in handling. There was no evidence of yielding of the structure.

The bulkheads for the pipe duct measurements were spun out of 0.025 in. of aluminum and were tried for fit in the concrete duct. They fit well and no rework is required. This completed the fabrication of the duct mockup.

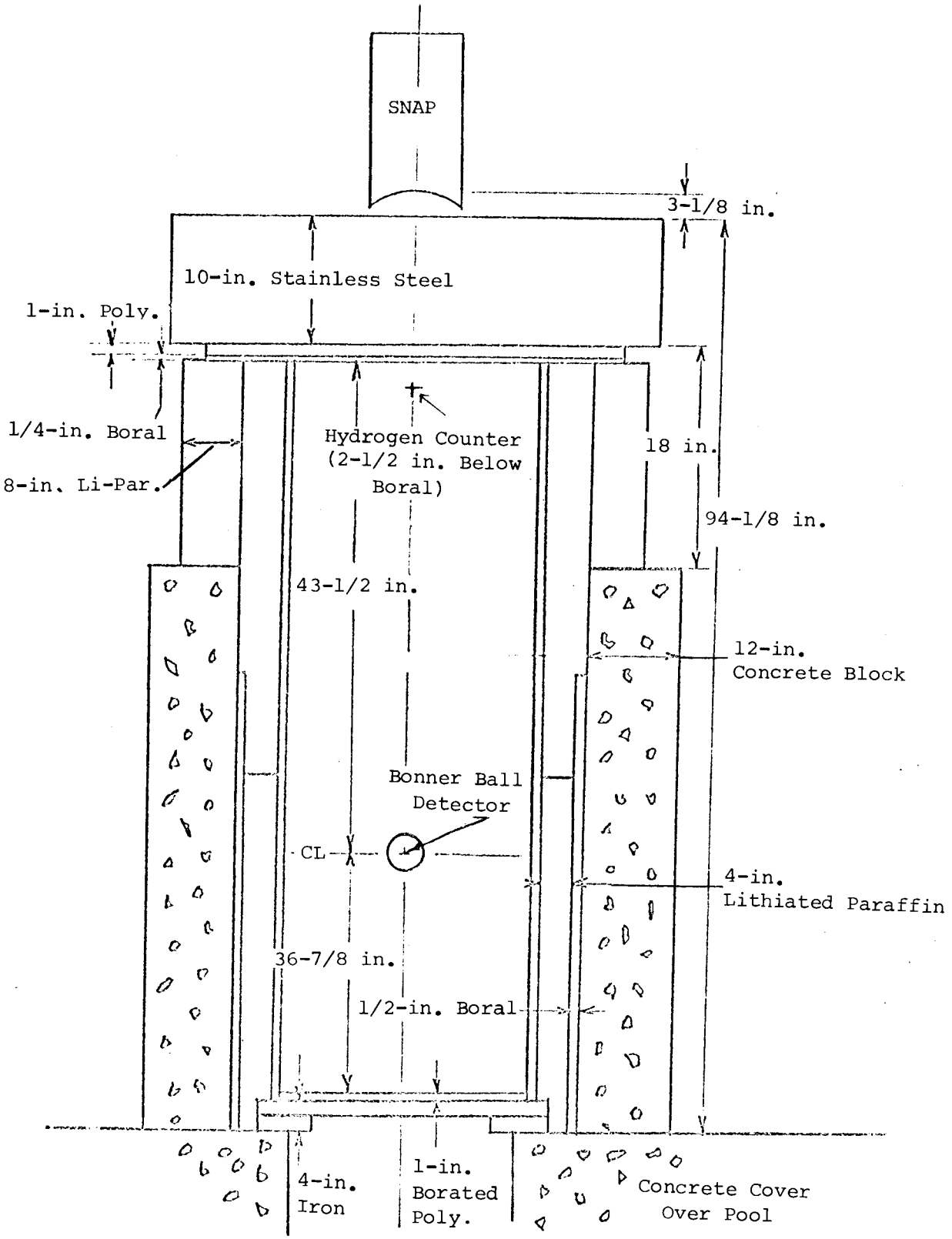

Fig. 1. Experimental Configuration No. 1

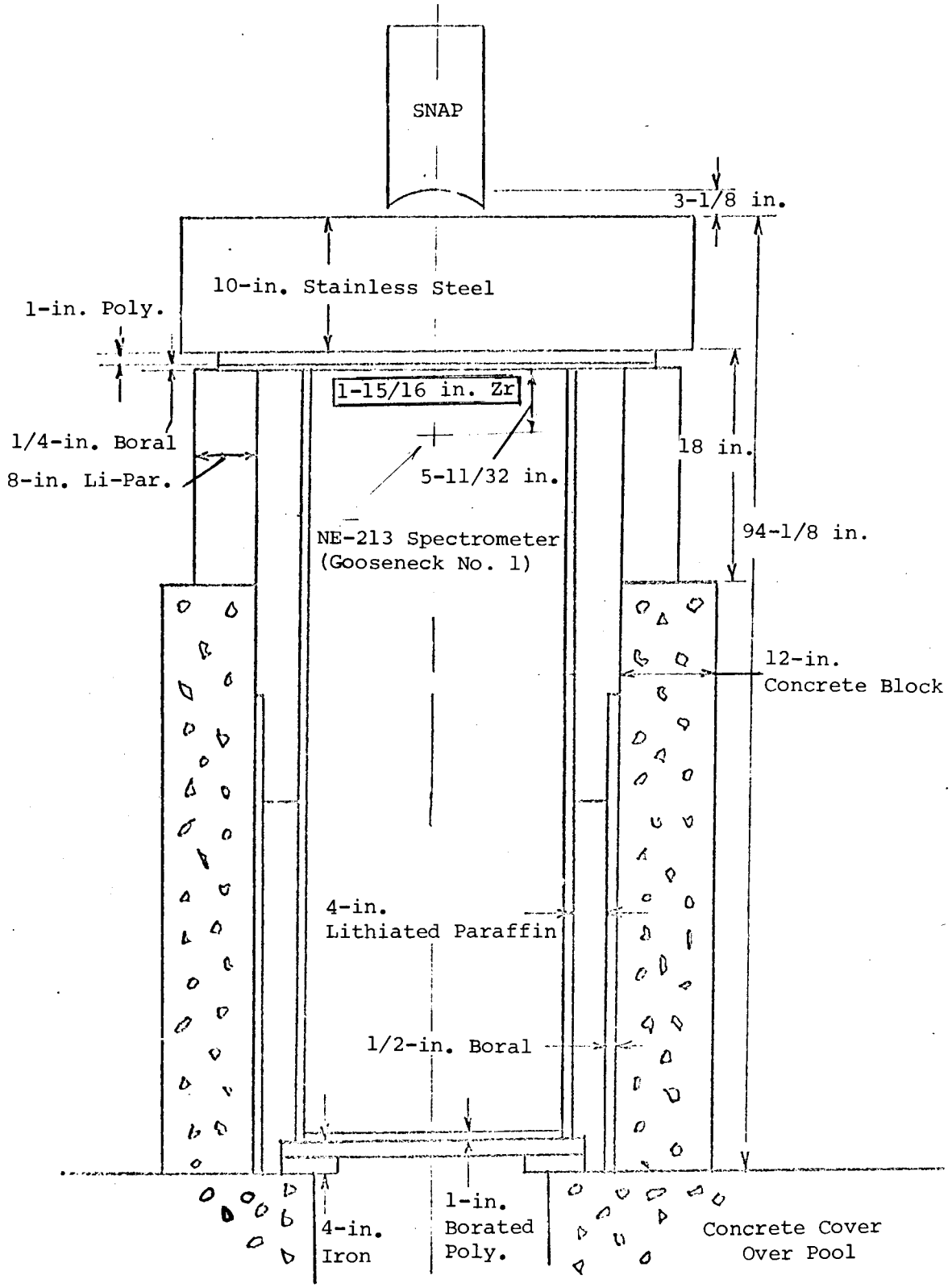

Fig. 2. Modified Configuration No. 1

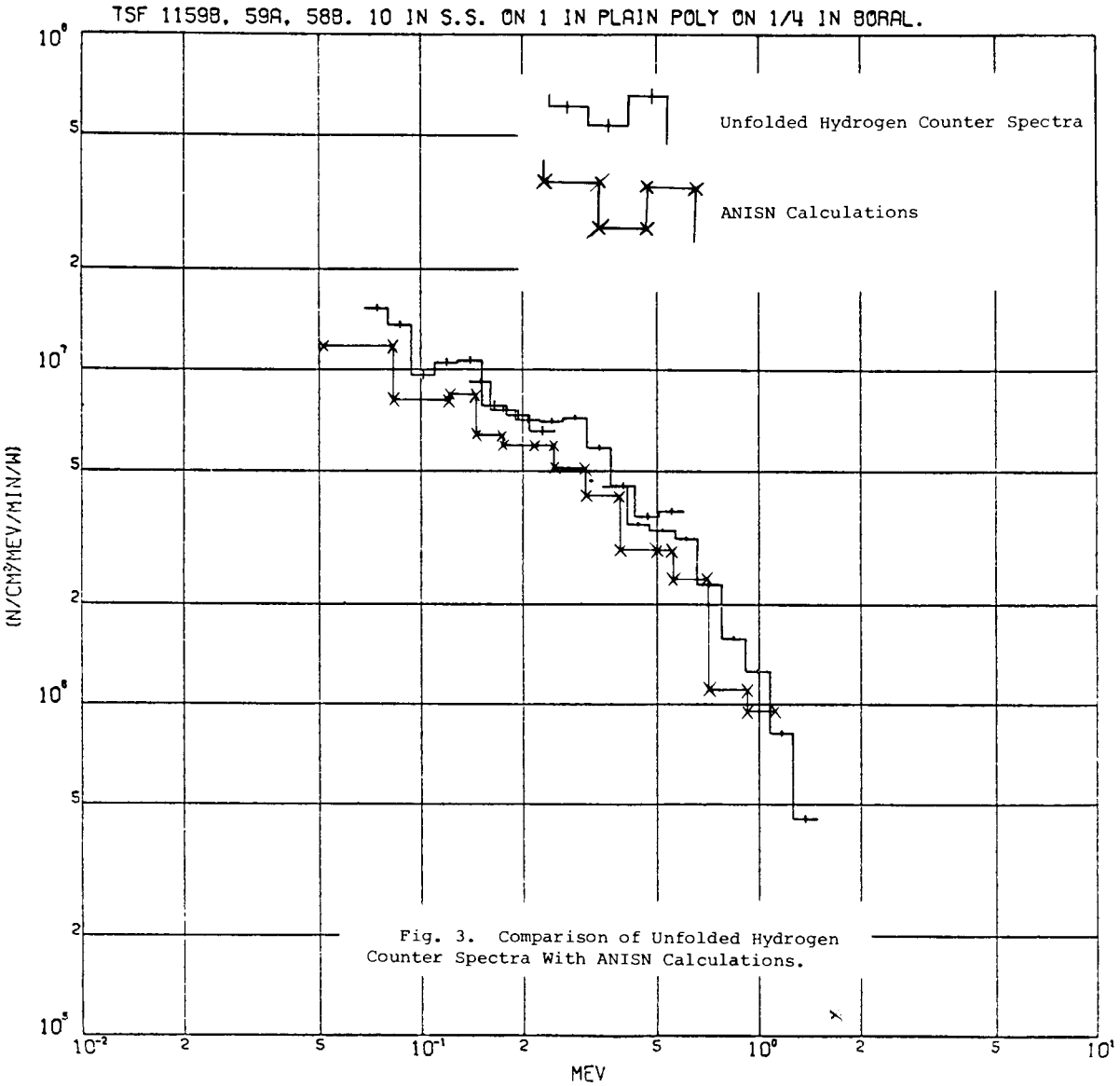

Fig. 3. Comparison of Unfolded Hydrogen Counter Spectra With ANISN Calculations.

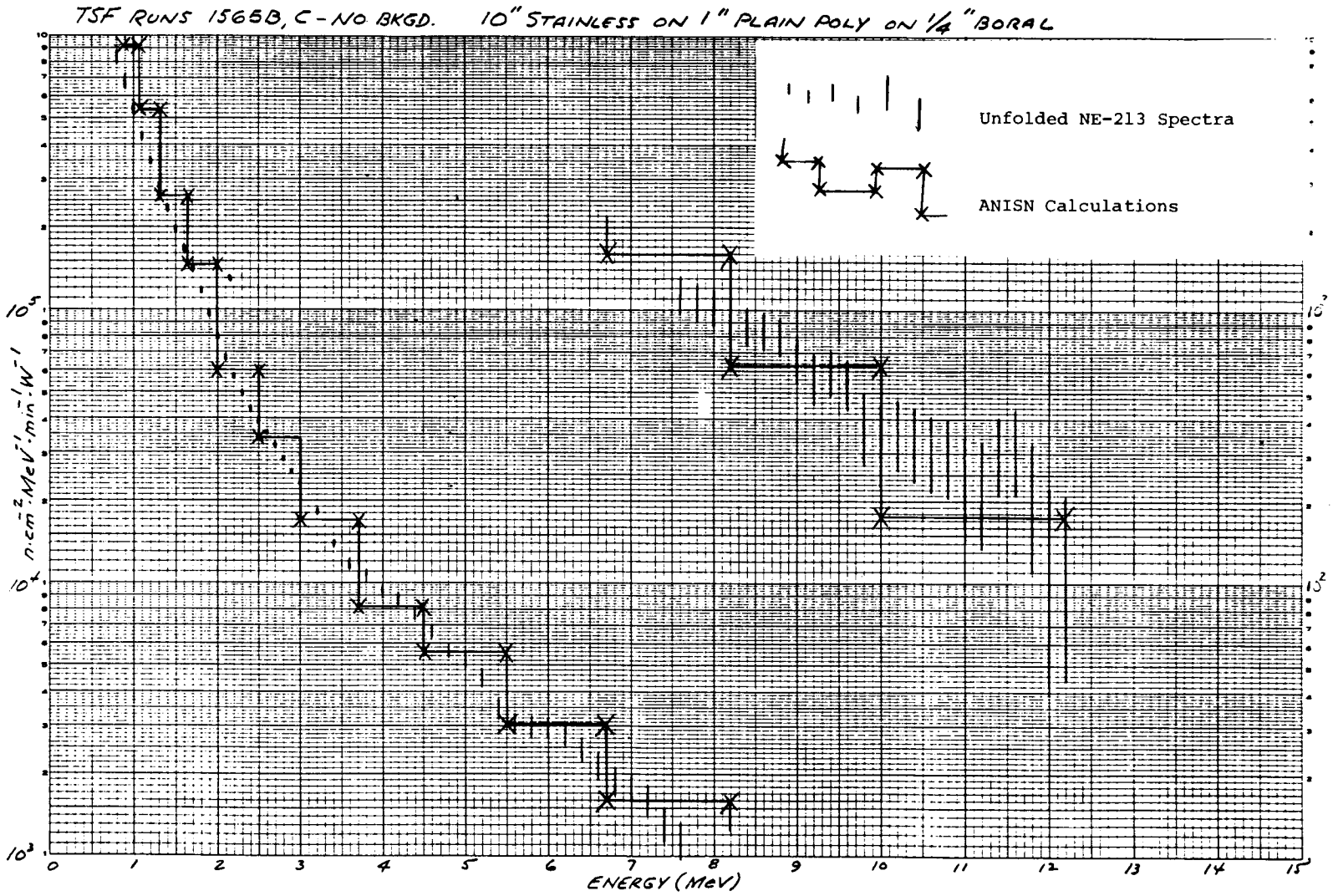

Fig. 4. Comparison of Unfolded NE-213 Spectra With ANISN Calculations.

Table 8. ANISN Modified-Source Calculations

Group	ΔU (lethargy)	ΔE (MeV)	Upper Energy (MeV)	Differential Flux As Calculated ($n/cm^2/sec/MeV$)	Differential Flux Normalized* to Experimental Spectra at 1 MeV ($n/cm^2/min/MeV/W$)
1	0.2	2.287(-7)	14.92	2.282(-7)	3.64(+1)
2	0.2	1.097(-6)	12.20	1.097(-6)	1.75(+2)
3	0.2	3.932(-6)	10.00	3.932(-6)	6.27(+2)
4	0.2	9.957(-6)	8.19	9.957(-6)	1.59(+3)
5	0.2	1.911(-5)	6.70	1.911(-5)	3.05(+3)
6	0.2	3.492(-5)	5.50	3.492(-4)	5.57(+3)
7	0.2	5.116(-5)	4.50	5.116(-5)	8.16(+3)
8	0.2	1.071(-4)	3.68	1.071(-4)	1.71(+4)
9	0.2	2.159(-4)	3.01	2.159(-4)	3.44(+4)
10	0.2	3.770(-4)	2.47	3.770(-4)	6.01(+4)
11	0.2	9.252(-4)	2.02	9.252(-4)	1.48(+5)
12	0.2	1.625(-3)	1.65	1.625(-3)	2.59(+5)
13	0.2	3.367(-3)	1.35	3.367(-3)	5.37(+5)
14	0.2	5.770(-3)	1.11	5.770(-3)	9.20(+5)
15	0.2	7.145(-3)	0.907	7.145(-3)	1.14(+6)
16	0.2	1.498(-2)	0.743	1.498(-2)	2.39(+6)
17	0.2	1.920(-2)	0.608	1.920(-2)	3.06(+6)
18	0.2	1.885(-2)	0.498	1.885(-2)	3.06(+6)
19	0.2	2.675(-2)	0.410	2.675(-2)	4.27(+6)
20	0.2	3.187(-2)	0.334	3.187(-2)	5.08(+6)
21	0.2	3.700(-2)	0.273	3.700(-2)	5.90(+6)
22	0.2	3.760(-2)	0.224	3.760(-2)	6.00(+6)
23	0.2	4.061(-2)	0.183	4.061(-2)	6.48(+6)
24	0.2	5.280(-2)	0.150	5.28(-2)	8.42(+6)
25	0.2	5.210(-2)	0.122	5.210(-2)	8.31(+6)
26	0.2	8.240(-2)	8.65(-2) 5.25(-2)	8.240(-2)	1.31(+7)

*$(n/cm^2/min/MeV/W) = C*(n/cm^2/sec/MeV)$, where $C = 1.594 \times 10^8$ sec/min/W. The normalized differential flux assumes a value of 9.2×10^5 $n/cm^2/min/MeV/W$ at 1 MeV; the average of the two experimental values at 1 MeV, 5.4×10^5 $n/cm^2/min/MeV/W$ for the NE-213 and 1.3×10^6 $n/cm^2/min/MeV/W$ for the hydrogen counter.

Table 9. Calculated Bonner Ball Count Rates* Vs. Measured For SNAP Spectrum Modifier, 10-in. Stainless Steel + 1-in. Poly. + 1/4-in. Boral

Detector	Measured (counts/minute/watt)	Calculated (counts/minute/watt)	Measured/Calculated
3-in. ball	773,560	588,638	1.31
3-in. ball	755,493	588,638	1.28
4-in. ball	1,846,450	1,628,431	1.13
5-in. ball	2,259,897	2,259,897**	1.0
5-in. ball	2,242,436	2,259,897	0.99
6-in. ball	2,144,601	2,230,572	0.96
8-in. ball	1,404,846	1,535,908	0.91
8-in. ball	1,394,554	1,535,908	0.91
10-in. ball	703,467	821,672	0.86
12-in. ball	315,454	391,894	0.80

* 50-group response functions from 123-group response functions calculated using newer ENDF/B polyethylene kernel data.

** Calculated results were normalized to the measurements for the 5-in. ball.

INTERNAL DISTRIBUTION

1-2. L. S. Abbott
3-7. C. E. Clifford
8. W. O. Harms
9. R. E. Maerker
10. F. C. Maienschein
11. F. J. Muckenthaler
12. F. R. Mynatt
13. A. H. Snell
14. D. B. Trauger
15. E. R. Cohen (consultant)
16. H. Feshbach (consultant)
17. H. Goldstein (consultant)
18. C. R. Mehl (consultant)
19. H. T. Motz (consultant)
20-21. Central Research Library
22. ORNL Y-12 Technical Library Document Reference Section
23-25. Laboratory Records
26. Laboratory Records ORNL RC
27. ORNL Patent Office

EXTERNAL DISTRIBUTION

28. R. Balent, Vice President, Power Systems Programs, Atomics International, P. O. Box 309, Canoga Park, Calif. 91304
29. W. L. Bunch, Radiation & Shield Analysis, WADCO, P. O. Box 1970, Richland, Wash. 99352
30. R. J. Creagan, Manager, LMFBR Project, Advanced Reactor Division, Westinghouse Electric Corp., Waltz Mill Site, P. O. Box 158, Madison, Pa. 15663
31. J. B. Dee, Head, GCFR Reactor Engineering, Gulf General Atomic, P. O. Box 608, San Diego, Calif. 92112
32. R. Ehrlich, Manager, Advanced Development Activity, Knolls Atomic Power Laboratory, General Electric, P. O. Box 1072, Schenectady, N. Y. 12301
33. L. F. Fidrych, Manager, Design Engineering, Breeder Reactor Development Operation, General Electric, 310 DeGuigne Drive, Sunnyvale, Calif. 94086
34. P. F. Fox, Westinghouse Electric Corp., Advanced Reactor Division, Waltz Mill Site, P. O. Box 158, Madison, Pa. 15663
35. W. H. Hannum, Division of Reactor Development and Technology, U. S. Atomic Energy Commission, Washington, D. C. 20545
36. P. B. Hemmig, Division of Reactor Development and Technology, U. S. Atomic Energy Commission, Washington, D. C. 20545
37. P. L. Havenstein, Chief, Instrumentation and Control Branch, U. S. Atomic Energy Commission, Washington, D. C. 20545
38. E. E. Kintner, Division of Reactor Development and Technology, U. S. Atomic Energy Commission, Washington, D. C. 20545
39. K. O. Laughon, USAEC Site Representative, ORNL
40. J. W. Lewellen, Division of Reactor Development and Technology, U. S. Atomic Energy Commission, Washington, D. C. 20545
41. T. E. Murley, Division of Reactor Development and Technology, U. S. Atomic Energy Commission, Washington, D. C. 20545
42. D. R. Riley, Chief, Core Design Branch, Division of Reactor Development and Technology, U. S. Atomic Energy Commission, Washington, D. C. 20545
43. E. E. Sinclair, Division of Reactor Development and Technology, U. S. Atomic Energy Commission, Washington, D. C. 20545

44. D. C. Spencer, Westinghouse Electric Corp., Advanced Reactor Division, Waltz Mill Site, P. O. Box 158,Madison, Pa. 15663
45. L. Strawbridge, Westinghouse Electric Corp., Advanced Reactor Division, Waltz Mill Site, P. O. Box 158, Madison, Pa. 15663
46. B. Wolfe, WADCO, P. O. Box 1970, Richland, Wash. 99352
47-48. Division of Technical Information Extension (DTIE)
49. Laboratory and University Division (ORO)